IOP Publishing Physica Scripta
Phys. Scr. 95 (2020) 045501 (8pp) https://doi.org/10.1088/1402-4896/ab1302

The mechanism of formation of desert mirages

Hongshou Li[1,2], **Rongmin Wang**[3] **and Hongtao Zhan**[1,2]

[1] Dunhuang Grottoes Monitoring Centre of Dunhuang Academy, Dunhuang 736200, Gansu, People's Republic of China
[2] Key Scientific Research Base of Conservation for Ancient Mural, State Administration for Cultural Heritage, Dunhuang 736200, Gansu, People's Republic of China
[3] Key Lab. Eco-Environment-Related Polymer Materials of Ministry of Education, College of Chemistry & Chemical Engineering, Northwest Normal University, Lanzhou 730070, People's Republic of China

E-mail: lihongshou@dha.ac.cn

Received 21 August 2018, revised 15 March 2019
Accepted for publication 25 March 2019
Published 11 February 2020

Abstract

The mirage is a unique optical phenomenon in the desert. This paper investigates the mechanism by which they form. Optical experiments in the Gobi show that the refractive index decreases about 20 to 40 cm above the ground causing a total reflection of ground surface light. Thus, ground light cannot get through and a 'water surface' mirage is formed—objects that are higher than the mirage will form an inverted image by reflection. Temperature and humidity monitoring prove that inversion of the refractive index occurs under the mirage. Mirage formation is mainly caused by temperature inversion in the 20 to 40 cm layer of the atmosphere, and phreatic water evaporation is the main reason for the formation of this temperature-inverted layer. The desert mirage is a phenomenon involving both total reflection and mirror reflection.

Keywords: desert mirage, phreatic evaporation, temperature, refraction

(Some figures may appear in colour only in the online journal)

1. Introduction

Travellers are often attracted by a fascinating 'lake' in the far distance when they drive through the Gobi desert. However, the lake disappears without trace if they try to get close to it. It is called the 'sea of mirage' in the sutra [1]. The Arabs called it 'the devil's sea' as it tempted thirsty people to wander towards their death. From times immemorial, this phenomenon has attracted the curiosity of a countless number of people [2–5]. The ancient Chinese believed that it was formed by water vapor, which was sprayed by an underground *long* (龙 *Chinese dragon)* [6].

Nowadays, a mirage is known to be a type of unique optical phenomena and is often described in physics textbooks as that when the air near the desert's surface is hot, the air density undergoes rarefaction. This leads to the air density and refractive index remaining high in the upper layer of air and low in the lower layer. There is a continuous variation in the refractive index formed and light that comes from a high and distant point is refracted upwards. Thus, an inverted image under the true object is formed, which is referred to as an 'inferior mirage' [7–11]. There are also 'superior mirages', which have a high refractive index in the low layer, and their formation follows the same principles, but has images that are upright, which have caused much debate over the years [12, 13].

At present, people pay more attention to the formation of object images than the formation of the mirage itself. Whatever the reason, the formation of the image of the '*sea surface*' of the mirage currently has no reasonable explanation. It may be that people think the phenomenon is too rare or inconvenient to monitor as most of the explanations considered are based on geometrical laboratory experiments [14–18], temperature and humidity profile analysis [19–26], or computer simulation [27–30]. They remain inadequately studied using practical monitoring methods and analysis [31].

Desert mirages are, in fact, not as rare. They are not only often seen in the Gobi desert, but can also be seen on asphalt roads [13, 32], where they look like water sprinkled on the road. In the Gobi region, near the world-famous Mogao Grottoes, mirages can be frequently seen. Based on our discovery and

Figure 1. A desert mirage and mirror in the test location.

studies [33–36], although the water table is deeper than 200 m, phreatic water evaporation exists [33–36]. It was found that the times and sizes of the appearance of mirages correlate remarkably with the times and intensities of phreatic water evaporation. The area of a mirage is larger at noon and the phreatic evaporation is also higher; the mirage is smaller in the morning and evening, and the evaporation is also low [34]. This observation led us to suspect there may be some inherent association between the formation of mirages and groundwater evaporation. Therefore, in this paper, we specifically devised optical experiments to monitor the refractive index of a mirage *in situ* to investigate the true mechanism responsible for its formation.

2. The study area

The experiment was performed in the Gobi region on top of the Mogao Grottoes in Dunhuang, northwestern China. The study area is located in landlocked hinterland. The climate is very dry, the annual rainfall is 42.2 mm, and potential evaporation is 4348 mm. The average annual temperature is 11.3 °C, the sunshine rate is 73%, and the solar radiation intensity can reach 1.1 kW m^{-2}. The average relative humidity (RH) is 31% and the average wind speed is 4.1 m s^{-1}. The soil porosity is 20%–30%. Recent research has shown that although the groundwater table is below 200 m, phreatic water evaporation is 0.0183 mm d^{-1} and has sinusoidal characteristics [33, 34]. Along with groundwater evaporation, mirages often appear in this area, as shown in figure 1.

3. Methods

As deeply-buried phreatic water evaporation has been discovered in the Gobi, we speculate that mirages may arise as a result of the water vapor. Firstly, the formation of the 'water surface' of the desert mirage was investigated to obtain the mirage's mechanism of formation. We primarily infer that *when light from the ground's surface moves upwards, the diminishing refractive index makes the light bend towards the ground, so total reflection occurs. As a consequence, the mirage's surface is also formed and the scene on the ground under the surface is not seen. Meanwhile, the inverted images of objects that are above the mirage are formed by reflection.*

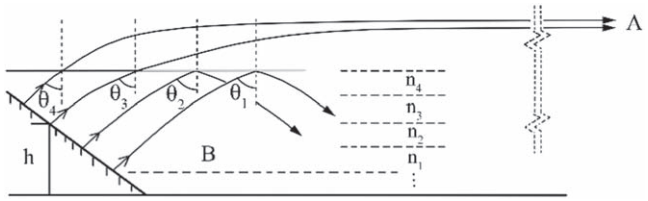

Figure 2. A sketch showing reflection from the mirror and the mirage formation route. (The light from the mirror bends downwards owing to $n_1 > n_2 > n_3 > n_4$, and makes the angle of incidence gradually increase ($\theta_4 < \theta_3 < \theta_2 < \theta_1$), when the angle is greater than the critical angle (θ_3), i.e. emitting light below h, the total reflective and forming mirage occurs (the gray line).)

Their formation mechanism is the same as in reflection from a real mirror's surface. If so, we can now perfectly explain the formation of the 'mirage water' and inverted image. To test this hypothesis, we carried out the following procedure.

(i) Point A (40°02′13.97521″ N, 94°47′38.28601″ E; elevation 1370.79 m), a site on the top of Mogao Grottoes, was selected on ground known to be a good site for mirage observation (figure 1). And point B (40°02″41.51953″ N, 94°47′46.36059″ E; elevation 1360.29 m) was selected in the central area of the mirage. Then, a glass mirror was used to reflect sunlight to point A, and we performed some optical tests. The actual observation point A′ was 1.45 m above A. A global positioning system measured the distance between A and B as 871.11 m and the altitude of the observation point at A is higher than B by 11.93 m.

If our above inference regarding optical paths is correct, then the phenomenon should certainly exist here: when a mirage appeared, we put a mirror at B, under the mirage's surface to a certain depth, at an angle to reflect sunlight to the observation site at A′, figure 2. No matter how the mirror's rotation angle was turned, the reflected sunshine could not be seen at the observation point A′ by eye. However, when there was no mirage, the same procedure allowed us to see the mirror's reflection of the sunshine.

Further details of the mirror experiment are as follows. When the mirage appeared, we used a plane mirror on a pedestal at point B to reflect sunlight to the observation point at A′ so that the reflected sunshine could be seen by eye. When the bright reflected light was observed, we fixed the angle of elevation of the mirror and moved a black-out cloth bag gradually downwards to shade the mirror (figure 3(a)) until no reflected sunshine could be seen from the mirror at the observation point, even by fully rotating a narrow glass mirror (figure 3(b)). Then, from the ground, we measured the vertical height (h in figure 2: the observer is below point A′, and the ground, which cannot be seen, is the vanishing line [37]) of the uncovered mirror. To make the test more convenient and reliable, the test could also be performed below height h using a narrow glass mirror and turning it around fully to check whether any light could pass through, figure 3(b). We repeated

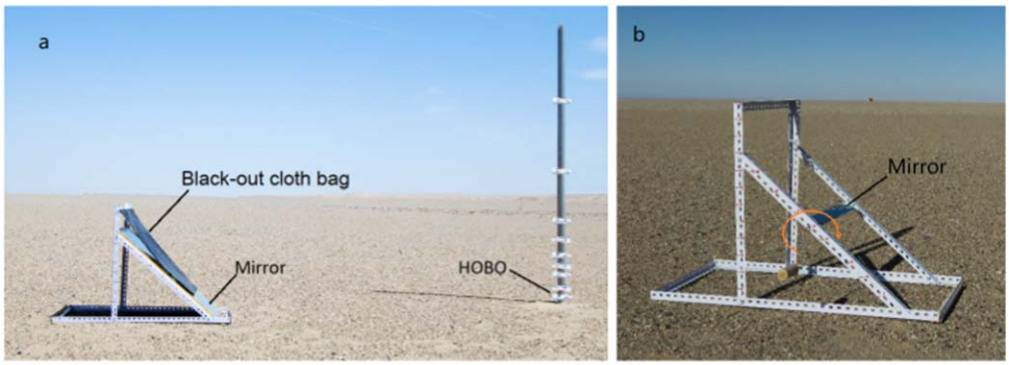

Figure 3. The experimental setup in the mirror experiment. (a) A black-out cloth bag was gradually moved downwards to shade the mirror to determine the height, and the HOBOs are removed shields to display the order, (b) rotating a narrow glass mirror to determine the height (h).

the measurement of h of the mirage at different times, and recorded the status of the mirage.

(i) Change in atmospheric refraction is a precondition for mirages to occur. The refractive index n is a function of temperature, humidity, and air pressure [32]. As the refractive index of the atmosphere is very close to that of a vacuum (i.e. 1), use refractivity N to express the refractive index n as $N = (n–1) \times 10^6$. The refractivity N is usually used instead of the refractive index [38]. Clearly, the higher the refractive index, the higher the refractivity. An empirical formula for refractivity is

$$N = 77.6\frac{P}{T} + 3.75 \times 10^5\frac{e}{T^2} \quad (1)$$

where T is the temperature (K), P is the pressure (hPa), and e is the vapor pressure (hPa). The latter can be written as $e = e_w\, RH$, where e_w is the saturated vapor pressure and RH is the relative humidity. An empirical formula for the saturated vapor pressure, as a function of altitude z, which is valid over the temperature range −30 °C to 60 °C, is [39]:

$$e_w = \mathrm{e}^{-z/7000} \times 6.1078 \times 10^{7.5t/(t+237.3)} \quad (2)$$

$$t = T - 273.16 \quad (3)$$

For B, the altitude z is 1360 m. The pressure differences caused by altitude differences in the mirage layer are very small and can been ignored. The daily pressure fluctuation also had no effect on the mirage inner layer sequence, and therefore we take the average atmosphere pressure to be 844 hPa during the experiments. Equations (2) and (3) are substituted into equation (1) and rearranged to give:

$$N = \frac{6.55 \times 10^4}{273.16 + t} + RH \times 1.958 \times 10^4 \times \frac{10^{\frac{7.5t}{t+237.3}}}{(273.16 + t)^2} \quad (4)$$

Thus, refractivity has been obtained as a function of temperature and RH. Thus, if we monitor the temperature and RH at point B, we can obtain the variation in the refractivity.

To obtain key evidence on mirages relating to the refractive index, we used mini-monitors (type HOBO-U23-001, the temperature is accurate to ±0.2 °C over the range 0 to 50 °C. RH in the range 0%–10% is accurate to ±4%; at 10%–90% it is accurate to ±2.5%. Resolution is 0.03%.) to monitor temperature and every 10 min in the central mirage area of point B at 5, 10, 20, 25, 30, 40, 50, 100, and 150 cm. Radiation shields shielded the loggers from direct solar radiation. The refractivity calculated from the recorded temperature and humidity data is used to reveal the mechanism responsible for forming the mirage.

At the same time, we produced a preliminary statistic on the mirage occurring time and frequency, and described the influencing factors, such as environmental temperature, RH, solar radiation, and wind speed according to the data (at 2 m height) of the weather station in the Gobi.

4. Results and analysis

4.1. Results of the optical experiments

After repeated observation, we found that mirages occurred approximately 3 h after sunrise and disappeared about 1 h before sunset (see table 1). The mirage's appearance time is associated with the time of day, along with the sunshine duration. They are more extended in summer, and the mirage emergence time is also earlier (and the vanishing time is later) than at other times. The situation is the opposite in winter. The non-reflecting vertical height (i.e. the maximum vertical height h) fluctuates with the emergence of the mirage: it rises slowly in the morning, reaches its highest value of 29 cm at noon, and subsequently gradually falls. The minimum height is 5 cm when the mirage vanishes. The area of the mirage surface and its height fluctuates from day to day, and can also change according to the height of the observer. When the observation point is raised, the mirage shrinks and may even vanish; when it is lowered, the mirage area expands. When h is lower than 5 cm, the light of the mirror no longer penetrates as the light is obstructed by the micro-topography around point B.

The experimental results prove that the total reflection forms the mirage. The explanation that the image of high objects is formed by the bending of light cannot be established at all. The gravel under the mirage cannot be observed when the mirage appears, which is consistent with the results

Table 1. Observation time, approximate non-reflecting vertical height h, and status of the mirage.

Time	h (cm)	Status of the mirage
After sunrise 1–2 h	5–14	No mirage formed. Scintillation gradually increasing. The Gobi gravel where the mirage will take place clearly seen.
After sunrise 2–3 h	14–19	Strong scintillation: the gravel is immersed in a small amount of the mirage.
Before and after noon	22–29	Mirage formed. Looks like a lake. Cannot see the gravel below the mirage. Strong winds shrink the lake and make the scintillation fluctuate intensely.
Before sunset 2 h	19–15	The mirage is shrinking and strong scintillation. Local gravel is exposed from the mirage and a sandbank is formed.
Before sunset 1 h	5–15	The mirage gradually disappears. The Gobi gravel is clearly seen, and the scintillation gradually weakens.

of the mirror experiment. Indeed, the light does not penetrate through the mirage, and the surface roughness is unrelated to formation of the desert mirage [40]. If the distant mirage was caused by light bending downwards, we should see the ground surface, and there would be no 'water surface' formed. Therefore, in the mirage, the optical paths are as shown in figure 2, and the refractive index decreases as one moves upwards ($n_1 > n_2 > n_3 > n_4$).

The lower the position of reflection on the mirror's surface, the more the reflected light bends to the ground in the process of passing through the 'water'. Therefore, we can be sure that $\theta_1 > \theta_2 > \theta_3 > \theta_4$. If θ_3 in figure 2 corresponds to the critical angle, then total reflection will occur. Therefore, when the mirror is covered to just below this level, an eye at the observation point at A′ will not receive reflected sunshine and the observer cannot see any light from the mirror even if the observer squats down. However, if the observer raises himself upwards, he can see light that has a path with an angle greater than the critical angle θ_3. The higher the point of observation, the brighter the light. The optical results fully correspond with previous analyses based on optical principles. However, whether or not there is evidence to be found in terms of the refractive index requires the support of the mirage monitoring data.

4.2. Temperature and humidity in desert mirages

The daily temperature, RH, absolute humidity, and refractivity in a typical mirage on Apr 28, 2010 were recorded and the results are shown in figure 4. It indicates that the air temperature rapidly rose after sunrise (figure 4(a)). At the same time, the RH rapidly decreased (figure 4(b)). However, the temperature and humidity at the different heights are only slightly different from 9:00 to 10:00 a.m. After 10:00 a.m., the surface temperature continues to rise due to the heating effect of the solar radiation. Over this period, the differences between the different layers are larger until about 1 h before sunset (19:00). In general, temperature decreases as one moves vertically upwards from 5 to 150 cm, and refractivity increases as described in textbooks. Therefore, the situation with respect to the refractive index does not match the desired variation $n_1 > n_2 > n_3 > n_4$ (figure 2).

However, after a careful survey, we found that there is a temperature inversion layer in the 20 to 40 cm band. Therefore, in contrast to the overall decrease in temperature with elevation, the temperature in this band behaves in the opposite manner, and therefore the refractive index undergoes inversion too. To observe this phenomenon more clearly, we 'enlarge' the local temperature and refractive index differences in figure 4(c). By retaining the main inverted layer and deleting unnecessary lines, a continuous inversion layer can be clearly seen, as shown in figure 5.

It was found that the temperature at a height of 25 cm is higher than that at 20 cm from 10:00 a.m. to 11:00 a.m. (figure 5(a)). Temperature at 40 cm also jumps higher than at 30 cm from 10:30 a.m. At 12:30, $T_{40cm} > T_{30cm} > T_{20cm}$, and this temperature inversion was continuous until 16:00. Then, the temperature at 40 cm declined, and the height of the inversion layer decreased. But, in the 25 to 30 cm range, inversion persisted until 18:10. The height of the temperature inversion layer clearly changes with the intensity of the solar radiation. It is higher around noon, and lower in the morning and evening. The mirage's depth (h) and surface area variation matches perfectly with the daytime increase and decrease of the solar radiation, as indicated in table 1.

The change in the refractive index differences is given in figure 5(b). It indicated the refractivity of the 20 cm layer is greater than that at 25 cm at 10:00 a.m. At 12:30, the refractivity at 25 cm starts to exceed that at 30 cm. From 16:30 to sunset, that of the 20 cm layer is higher than that at 25 cm. Meanwhile, that of the 40 cm layer is greater than that at 50 cm from 16:00 to 20:00. There are double inverted layers. Therefore, there is an inversion refractivity layer in the whole. The height changes in the refractive index differences are consistent with the measured heights of the mirage given in table 1. They are slightly lower than the height of the temperature inversion layer and are in complete agreement with the optical principle of total reflection. Theoretically, once inversion of temperature or the refractive index occurs, a desert mirage would be formed and would be observed at an appropriate location.

According to our monitoring, it was found that if there is no inversion in the temperature and refractivity, there is no mirage, and the refractivity increases in an orderly fashion in the upwards direction, while the temperature decreases. This strongly supports the previous analysis. By repeating our experiments, it completely excluded the possibility that our

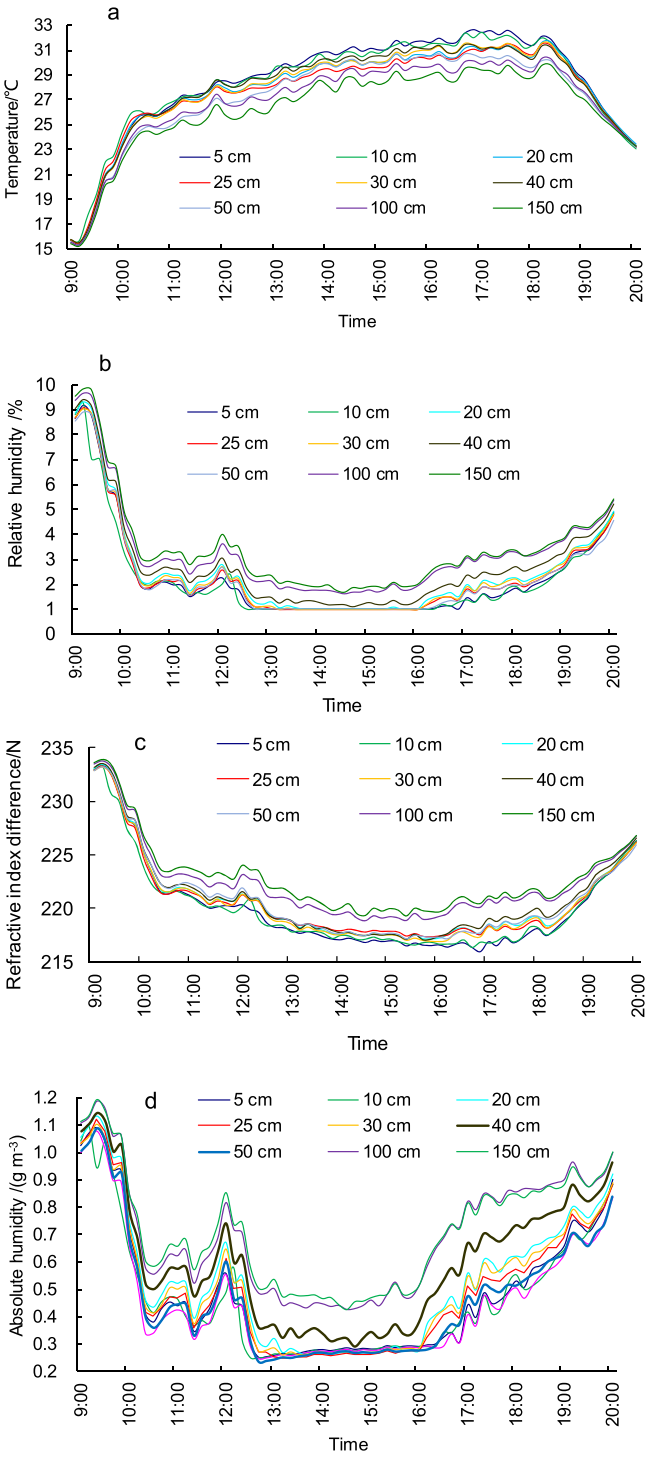

Figure 4. The temperature (a), RH (b), refractivity (c), and absolute humidity (d) at different times of day at different heights in a typical desert mirage.

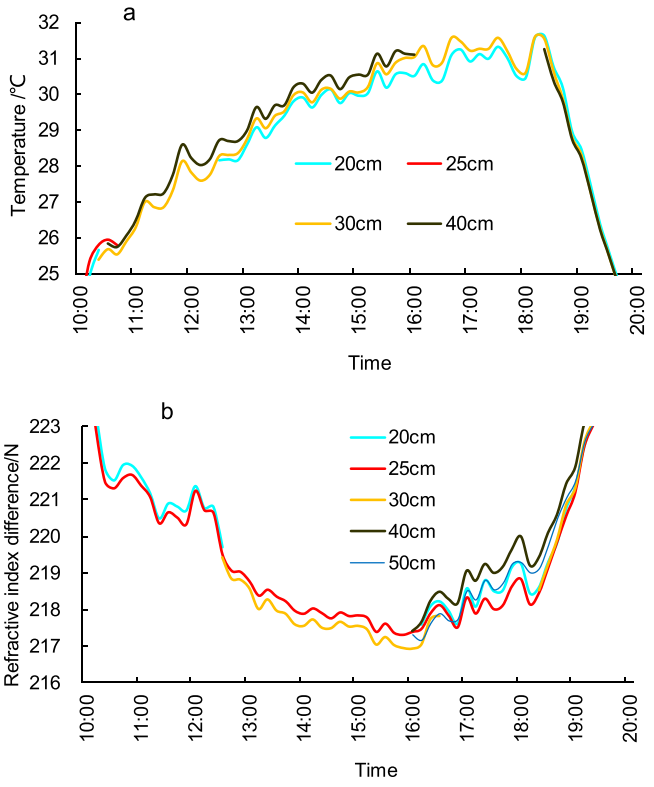

Figure 5. Temperature (a) and refractive index (b) inversion in the desert mirage monitoring data.

results were erroneous due to instrumental, operator, or systematic errors, or limitations in the precision of the apparatus. Therefore, both the optical and refractive index monitoring experiments proved that the optical mechanism responsible for desert mirages involves total reflection in ~40 cm.

In equation (4), the two terms on the right-hand side of the equation, $6.55 \times 10^4/(273.16 + t)$ and $1.958 \times 10^4[10^{7.5t/(t+237.3)}]RH/(273.16 + t)^2$, correspond to the contributions to the refractivity made by dry air (i.e. when RH = 0) and by the presence of water vapor, respectively [32]. In figure 4(c), such as 30 cm, the average value ($t = 27.8$ °C) of the dry-air contribution is 217.6, while the average contribution of the water vapor (RH = 2.4%) is 2.7. Obviously, the two contributions are not of the same order of magnitude—the humidity features as a fine adjustment to the refractivity differences between layers. From a comparison of the refractivity differences and temperature in figure 5, the change in refractivity difference does not completely tally with the temperature changes. Obviously, it is not that the temperature caused changes in the air density and refractive index and resulted in a mirage, as is the explanation given in textbooks.

A mirage is a total reflection phenomenon. Under the mirage, temperature inversion forms a mirage surface, and mirror-like reflection forms an inverted virtual image [20]. Above the inversion layer, there is a decrease in temperature with height, which automatically produces a gradient of index of refraction that can lead to curved parallel light rays [31], i.e. above the inversion layer; no total reflex occurred there.

However, the root cause of the temperature inversion is worth further exploration. The absolute humidity variation is shown in figure 4(d). At a height of 40 cm, a stable layer with relatively high-water vapor density can be seen to have formed. Moreover, after carefully examining the variation in RH in figure 4(b), we find it is also higher at 40 cm. Therefore, there is a high humidity level above the mirage's surface, which, obviously, must be related to phreatic water evaporation [33]. When both phreatic water evaporation and

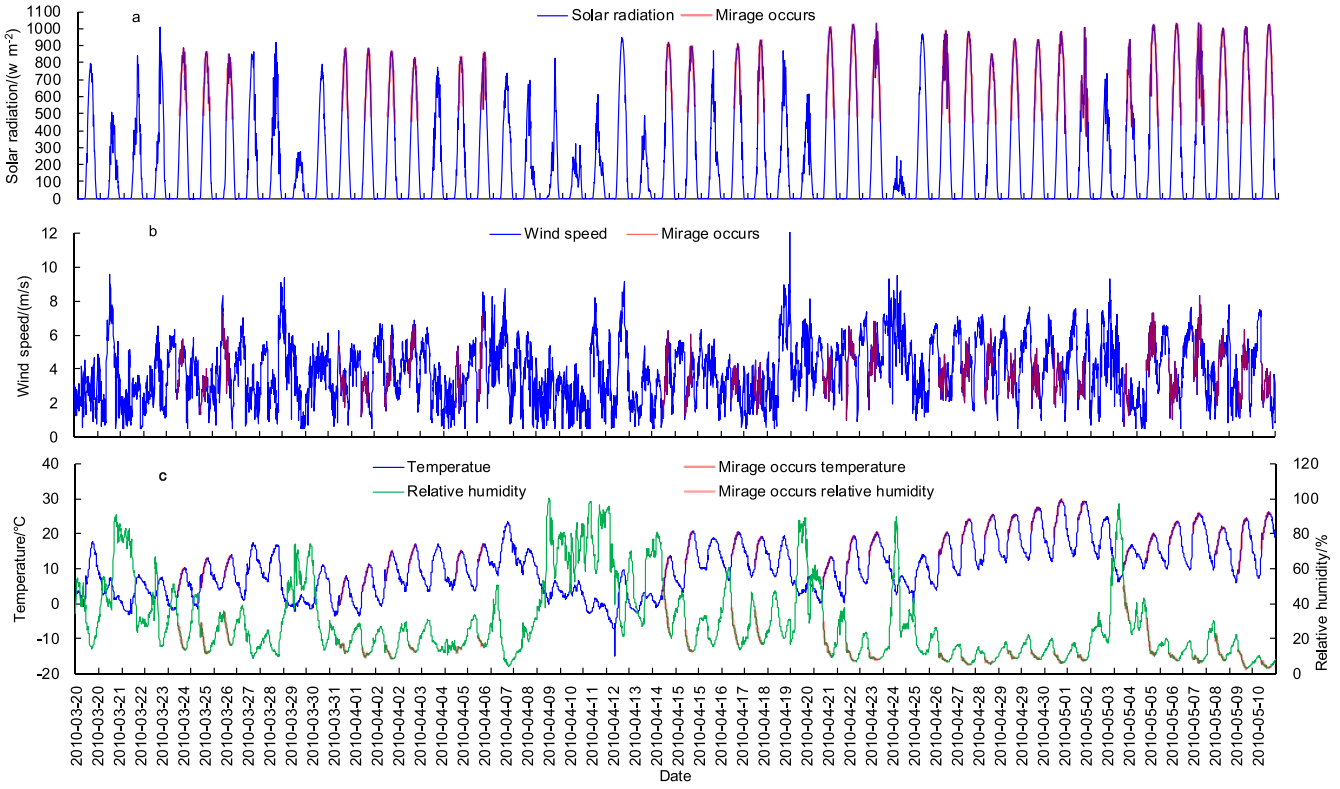

Figure 6. The mirage occurrence time, frequency and the corresponding solar radiation (a), wind speed (b), temperature and RH (c).

mirages occur, the diversity between the moisture in the 40 cm layer and the neighboring ones is significant. Water vapor is a greenhouse gas. In the process of phreatic water evaporation from the ground, the vapor absorbs the long-wave radiation, makes the temperature rise and forms the temperature inversion layer. Thus, a layer is formed at 40 cm with locally higher water content and this leads to temperature and refractive index inversion. On the other hand, the horizontal wind blown on the surface may have a beneficial effect on the formation of the humidity inversion layer. Therefore, the ancient Chinese explained the formation of mirages with a simple and visualized glossary, earth-air (地气 *Di-qi*), which means *Long* (*Chinese dragon*) spraying water vapor. And it is the most accurate explanation of mirages in ancient civilization. The earth-air comes from soil released water vapor and air. It has been extensively monitored by the ancient Chinese. However, owing to the fact that the monitoring method of '候气 *Hou-qi*' has been lost, this explanation was misunderstood as superstition for a long time [33–36].

5. Discussion

Here, the first conclusion is that water vapor is one of the basic ingredients of the mirage. Desert mirages in particular are a product of phreatic water evaporation [33–36] combined with the arid climate. The area of desert mirage is positively correlated with the sinusoidal phreatic evaporation [34]. On sunny days with high phreatic evaporation and dry atmosphere (figure 6(a)), it is favorable to forming an inversion layer of humidity, temperature and refractivity. According to our observations, mirages do not form on days that are cloudy and in dusty weather, meanwhile, there is almost no evaporation [33, 34]. In these conditions, temperature and refractive index inversion does not occur and, of course, there is no mirage formation. A mirage's probability of occurrence (∼40%) is much smaller than the sunshine probability rate (∼73%), according to incomplete statistics. The occurrence frequency in winter and spring is significantly lower than that in summer and autumn, and the sizes are also smaller in winter and spring.

Thus, it would be very difficult to form a temperature inversion layer in arid areas without groundwater evaporation. Phreatic water evaporation is, therefore, a necessary condition for mirage formation. Conversely, the desert mirage is an important indicator of phreatic water evaporation. The observation shows that the mirage disappears (figure 5(a)) when the atmosphere temperature begins to drop (figure 6(c)). We infer that the shallow layer soil temperature drops to a critical point; at this time, the soil absorbs enough vapor [33] resulting in a reduction in evaporation and the reverse layer disappears.

Topography has an important impact on mirage formation as well. The depth of the mirage is shallow, less than 40 cm. Even if vapor is present, temperature inversion occurs, and without a suitable observation point, the mirage will not be seen. The sky and mountain are reflected on the mirage and have an important effect on the color and brightness of the mirage. Mirages are usually formed in areas that are

slightly concave. Low-lying terrain can effectively reduce the speed of the wind near the ground, and this is conducive to formation of a temperature inversion layer. The wind's average speed is 4.3 m s^{-1} during data monitoring in figure 4. This modest wind speed does not generally affect the formation of a mirage; low wind speed (figure 6(b)) may benefit formation of a desert mirage [41], but in stronger winds (>8 m s^{-1}) the mirage 'water' will be essentially blown away, revealing a sandy bottom and making strong scintillation visible.

Therefore, the desert mirage is a synergetic phenomenon involving many factors [20]. Several environmental factors, such as temperature [42–46], water vapor [22–26], CO_2 [47], solar radiation intensity, wind speed [40], micro-landform, and even observation location, are very important in mirage formation.

Let us return to mirages that appear on asphalt roads. We suggest that the mechanism of formation in this case is essentially the same, the only difference being that the temperature inversion layer is much thinner (Zhou *et al* measured it to be no more than 5 mm, even in summer [13]). In this case, the greenhouse gas that forms the temperature inversion layer may not be moisture but volatile organic compounds from the asphalt. With the high temperatures and strong sunlight in summer, the polymer chains in the asphalt may be decomposed. The volatilized gases so formed have a strong ability to absorb long-wavelength thermal infrared radiation, and thus temperature inversion and mirages can be formed as well. Therefore, mirages will form more readily in the high temperatures encountered in summer and on newer asphalt roads.

6. Conclusions

Using optical tests, and by monitoring the temperature and humidity of a mirage in the field, the mechanism of formation of desert mirages has been revealed. As water vapor rises, the vapor absorbs heat. This creates a temperature inversion layer and the refractive index diminishes in the upwards direction. As a result, the light emitted from the ground undergoes total reflection below ~40 cm corresponding to the mirage's surface. Consequently, the surface of the ground underneath the mirage cannot be seen. The objects above the mirage are reflected, which is completely analogous to the principle of reflection from a mirror. Water vapor is critical for the formation of the temperature inversion layer. The desert mirage is a form of earth-air activities and a part of Chinese dragon cultures. It is important for people to understand these peculiar optical phenomena scientifically.

Acknowledgments

We gratefully acknowledge funding from the National Natural Science Foundation of China (41967029; 41363009); The Gansu Province Science and Technology Plan (1308RJZF290).

ORCID iDs

Hongshou Li https://orcid.org/0000-0001-8588-122X

References

[1] Gemmel W (ed) 1998 *Diamond Sutra Or Prajna-Paramita* (Beau Bassin: Kessinger Publishing)
[2] Mallock A 1928 Mirage: natural and artificial *Nature* **122** 94–5
[3] Raman C V and Pancharatnam S 1959 The optics of mirages *Proc. Indian Acad. Sci.* A **49** 251–61
[4] Tape W 1985 The topology of mirages *Sci. Am.* **252** 125–30
[5] Khular E, Thyagarajan K and Ghatak A 1997 A note on mirage formation *Am. J. Phys.* **45** 90–2
[6] Sheng K and Bi Tan M X 2013 *Chinese Science Encyclopedia* (Shenyang: Wanjuan Publishing Company; North united publishing media co., Ltd) pp 223–4
[7] Lemons D S 1997 *Perfect Form: Variational Principles, Methods, and Applications in Elementary Physics.* (New Jersey: Princeton University Press) pp 33–7
[8] Thomas T W 2008 *Desert Meteorology* ed W Wei, C Cui and H Shang (Beijing: China Metorological Press) pp 386–8
[9] Gove P B 1964 Webster's third new *International Dictionary of the English Language Unabridged* (Springfield, Massachusetts: G & C Merriam Company) p 1441
[10] Young A T and Frappa E 2017 Mirages at Lake Geneva: the fata morgana *Appl. Opt.* **56** G59–68
[11] Tränkle E 1998 Simulation of inferior mirages observed at the Halligen Sea *Appl. Opt.* **37** 1495–505
[12] Fabri E, Fiorio G, Lazzeri L and Violino P 1982 Mirage in the laboratory *Am. J. Phys.* **50** 517–28
[13] Zhou H C, Huang Z F, Cheng Q, Lu W, Qiu K, Chen C and Hsu P F 2011 Road surface mirage: a bunch of hot air? *Chinese Sci. Bull.* **56** 962–8
[14] Vollmer M and Tammer R 1998 Laboratory experiments in atmospheric optics *Appl. Opt.* **37** 1557–68
[15] Young A T 2015 Inferior mirages: an improved model *Appl. Opt.* **54** B170–6
[16] Vollmer M 2009 Mirrors in the air: mirages in nature and in the laboratory *Phys. Educ.* **44** 165–74
[17] Greenler R G 1987 Laboratory simulation of inferior and superior mirages *Opt. Soc. Am.* A **4** 589–90
[18] Gutierrez D, Seron F J, Munoz A and Anson O 2006 Simulation of atomospheric phenomenona *Comput Graph-UK* **30** 994–1010
[19] Birch K P and Downs M J 1988 The results of a comparison between calculated and measured values of the refractive index of air *J. Phys. E: Sci. Instrum.* **21** 694–5
[20] Woyk E 1978 Ray tracing theory and mirage occurrence conditions *Appl. Opt.* **17** 2108–13
[21] Lehn W H and Friesen W 1992 Simulation of mirages *Appl. Opt.* **31** 1267–73
[22] Colavita M M, Swain M R, Akeson R L, Koresko C D and Hill R J 2004 Effects of atmospheric water vapor on infrared interferometry *Pub. Astron. Soc. Pacific* **116** 876–85
[23] Mathar R J 2007 Refractive index of humid air in the infrared: Model fits *J. Optics A: Pure Appl. Opt.* **9** 470–6
[24] Vollmer M, Shaw J A and Nugent P W 2015 Visible and invisible mirages: comparing inferior mirages in the visible and thermal infrared *Appl. Opt.* **54** B76–84
[25] Edlén B 1966 The refractive index of air *Metrologia* **2** 71–80
[26] Beers J and Doiron T 1992 Verification of revised water vapour correction to the refractive index of air *Metrologia* **29** 315–6
[27] Musgrave F K and Berger M 1990 A note on ray tracing mirages *IEEE Comput. Graph. Appl.* **10** 10–2

[28] Berger M, Trout T and Levit N 1990 Ray tracing mirages *IEEE Comput. Graph. Appl.* **10** 36–41
[29] Lu J and Zhou H C 2017 Numerical reproduction and explanation of road surface mirages under grazing-angle scattering *Appl. Opt.* **56** 5550–8
[30] Yang Z and Vorontsov M A 2015 Numerical analysis of mirage-image formation in presence of atmospheric turbulence and refractive gradient layer *Imaging and Applied Optics 2015 OSA Technical Digest (online) paper PM4C.4*. Optical Society of America (https://doi.org/10.1364/PCDVTAP.2015.PM4C.4)
[31] Tavassoly M T, Osanloo S and Salehpour A 2015 Mirage is an image in a flat ground surface *J. Opt. Soc. Am.* A **32** 599–603
[32] McNair F W 1920 A sidewalk mirage *Science* **52** 201
[33] Li H S, Wang W F and Liu B L 2014 The daily evaporation characteristics of deeply buried phreatic water in an extremely arid region *J. Hydr.* **514** 172–9
[34] Li H S, Wang W F, Zhan H T, Qiu F, Wu F S and Zhang G B 2017 Measurement and analysis of the yearly characteristics of deep-buried phreatic evaporation in a hyper-arid area *Acta Ecol. Sin.* **37** 53–9
[35] Li H S and Zhan H T 2018 The characteristics and mechanism of formation of earth-air pulsation in extremely arid areas *J. Geophys. Res.: Atmospheres* (https://doi.org/10.1029/2018JD028870)
[36] Li H S 2018 Exploring the source and potential of Earth-air pulsation using a closed system *Earth Interact.* (https://doi.org/10.1175/EI-D-17-0019.1)
[37] Greenler R 1980 *Rainbows, Halos, and Glories* (Cambridge: Cambridge University Press)
[38] Liu Z Z, Liu J N and Li Z H 2000 The application of GPS technology to meteorology *Bull. Surv. Mapp.* **2** 7–8
[39] Temp, Humidity & Dew Point ONA. (http://faqs.org/faqs/meteorology/temp-dewpoint/)
[40] Tavassoly M T, Nahal A and Ebadi Z 2004 Image formation in rough surfaces *Opt. Commun.* **238** 252–60
[41] Paulson C A 1970 The mathematical representation of wind speed and temperature profiles in the unstable atmospheric surface layer *J. Appl. Meteorol.* **9** 857–61
[42] Benoit R 1977 On the integral of the surface layer profile-gradient functions *J. Appl. Meteorol.* **16** 859–60
[43] Högström U 1996 Review of some basic characteristics of the atmospheric surface layer *Boundary-Layer Meteorol.* **78** 215–46
[44] Singh R N, Negi S S, Sahay A K, Singh A, Varughese K O G and Walia A K 1994 Mirage formation in the thermal region *Appl. Opt.* **33** 3279–80
[45] Fraser A B 1979 Simple solution for obtaining a temperature profile from the inferior mirage *Appl. Opt.* **18** 1724–31
[46] Mach W H and Fraser A B 1979 Inversion of optical data to obtain a micrometeorological temperature profile *Appl. Opt.* **18** 1715–23
[47] Jatin P J and Erhard W R 2005 Superior mirage effect in supercritical CO^2: experiment and model *J. Supercrit. Fluid.* **35** 260–4